The Finite Elements Analysis on Magnetic Field of Controllable Saturated Reactor

Wang Ziqiang, Yin Zhongdong, Yang Po, Li Ke
Key Laboratory of Power System Protection and Dynamic Security Monitoring and Control of Ministry of Education
North China Electric Power University
Beijing, China
E-mail: wangzq_ken@163.com

***Abstract*—In the power system, the controllable reactor can be used as reactive power compensation device to limit over-voltage operation, reduce no-load or light load loss and improve transmission capacity. It is with characters of simple structure, easy maintaining, low cost and high stability, etc. The magnetic field is closely related to the reactor performance. In this paper, aiming at a controllable saturated reactor prototype, using the finite elements method, the magnetic field is studied. Then, the precise 2-D prototype field-circuit coupling model is established based on the magnetic field analysis and the finite element analysis software - ANSYS. Using this model, the magnetic field and working currents concrete values under the condition that AC and DC excitations co-exist within the core are calculated. The analysis results indicate that finite element analysis theory can effectively analyze the magnetic field of the reactor.**

Keywords-magnetic field; controllable saturated reactor; finite elements theory

I. INTRODUCTION

Finite element method (FEM) is a numerical method which is used to approximately solve the general problem of continuous fields. In 1943, the basic idea of the finite element theory was proposed by R.Courant for the first time, and this theory has been continuously improved by scholars, with a rapid progress. Finite element theory which is originated in the structural analysis theory has been gradually used in the Electromagnetic field analysis after its theory and formula are improved and promoted [1].

The finite element analysis software ANSYS can be used to conduct electromagnetic calculation, solve the problem on the distribution of magnetic field in a particular device or a certain component. Maxwell equations are the starting point of the electromagnetic analysis. The unknown value (DOF) that mainly calculated in the finite element method is magnetic potential or electric potential. Other issues, such as magnetic flux density, current density, energy, force, loss, inductance and capacitance can be derived from these unknown values [2].

Saturated reactor is a kind of nonlinear circuit with iron core, DC and AC windings. It controls saturation degree of the iron core by using of the DC excitation, thus changes the reactance of the AC winding. The field-circuit coupling model of the saturated reactor refers to the model of taking account of the external circuit and the magnetic field within the iron core.

II. CORE STRUCTURE AND MAGNETIC FIELD ANALYSES

A. Core Structure of Saturated Reactor

The magnetic properties of iron core are related to ferromagnetic materials, iron core structure and manufacturing process. Therefore, suitable magnetic materials should be chosen. Magnetic materials used now are Fe-Ni alloy and cold-rolled silicon sheet. The eddy current should be taken into account when choosing the thickness of the iron core material in order to reduce the iron loss and limit the temperature rise. Comprehensive consideration suggests that *0.3-0.35mm* is the optimal choice considering the fact that the thinner the magnetic material, the lower some properties will be. The reactor prototype studied in this paper uses cold-rolled non-oriented silicon steel sheet, with a thickness of *0.35mm*.

Besides, in order to make full use of the magnetic properties of iron core, it is necessary to choose a reasonable structure and size ratio. Non-uniform magnetization occurs, air gap exists in the magnetic circuit, or individual magnetization direction of the magnetic circuit is different from the easiest magnetization direction of the material can affect the iron core's magnetic properties. In the choice of core structure and its geometry size, the inherent magnetic properties should be made full use of. And at the same time, smallest geometry size and lightest weight should be pursued in the premise of technical requirements. Finally, easy to manufacture and economic cost should be considered also. Above all, the core structure of the saturated reactor and the external circuit are as follows:

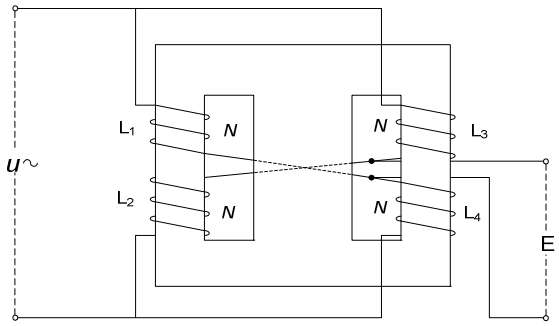

Figure 1. Core structure and circuit.

This work was supported by the China National Natural Science Fund (50777019) and National Mega-projects of Science and Technology for the 11th Five-year Plan (2007BAA12B03).

In Fig.1, the primary core of the reactor is divided into identical two parts which have the same cross-section area. Furthermore, the cross-section area of the middle yoke is twice times as much as a side core. Four windings, with the same turns of *N*, are symmetrically winded on the two side core columns respectively. At the same time, the upper and lower windings distributed on different columns are cross connected to form two circuits which are in parallel connection. Then they are all connected to the network source *U*. Besides, the two nodes in the middle of the branches are connected to DC control source *E*.

When the saturated reactor works, the control actions are performed by DC excitation, and therefore the DC control winding is also called controlling winding. At the same time, the AC winding (work winding) is connected with the load. When the DC excitation current doesn't exist, the inductance of the AC winding is the largest and the current is the smallest. This state is equivalent to the no-load transformer. When DC excitation maintains unchanged, the DC and AC components of the magnetic induction coexist in the iron core. Because of the additive effect of AC and DC excitation, the core will work on the saturation state of magnetic property. Therefore, AC magnetic field intensity increases and the core's equivalent permeability decreases at the same time [3]. The more saturated the iron core, the smaller the permeability and the reactance of non-linear reactor will be. When the voltage of the power source keeps invariant, the reactance will keep constant too. And in this case, the reactor is uncontrollable.

B. Magnetic Field Analysis of The Core Magnetic Field

The finite element calculation method, used in the magnetic field of saturated reactor iron core, is a extremum problem that converts boundary value problems on differential equations of magnetic field into equivalent energy functional. Then field domain is discretized into finite units, and in each unit the unknown functions are expressed by interpolating functions with unknown coefficients. By substituting the interpolating function into the integral formula of energy functional, the functional is discretized into ordinary multivariate function. According to the principle of extremum problems on multivariate function, partial derivations of each variable in the energy function are solved. Through making the results equal to zero, linear or non-linear equations will be got [4].

The saturated reactor works under the frequency of 50Hz, so the magnetic field is the low frequency steady alternating magnetic field. All of the points in each unit have the same magnetic field intensity. After the displacement currents are neglected, Maxwell Equations of the reactor can be expressed as follows:

$$\nabla\times E=-\frac{\partial B}{\partial t} \tag{1}$$

$$\nabla\times H=J \tag{2}$$

$$\nabla\cdot B=0 \tag{3}$$

Where, $\nabla\times$ and $\nabla\cdot$ is respectively curl operator and divergence operator; H is magnetic field intensity vector; J is current density vector; E is electric density vector; B is magnetic flux density. The relationships among these field quantities are as follows: $D=\varepsilon E$, $B=\mu H$, $J=\sigma E$. Where, D, ε, μ and δ is respectively electric displacement vector, dielectric constant, permeability and conductivity.In order to reduce the number of the unknown quantities, magnetic vector potential A and electric scalar potential φ are introduced.

$$B=\nabla\times A \tag{4}$$

Substituting the equation (4) into (2), differential equation of the magnetic vector potential can be expressed as follows:

$$\nabla\times\frac{1}{\mu}\nabla\times A=J \tag{5}$$

Integrating the first and the second class boundary conditions, the boundary value problem represented by magnetic vector potential A can be expressed as follows:

$$\begin{cases}\nabla\times\left(\dfrac{1}{\mu}\nabla\times A\right)=J\\ \Gamma_1: A=A_0\\ \Gamma_2:\dfrac{1}{\mu}\nabla\times A\times n=0\end{cases} \tag{6}$$

The variational problems equivalent to formula（5）can be expressed as follows:

$$\begin{cases}\Omega:\min I(A)=\int_\Omega\dfrac{1}{2}H\cdot Bd\Omega-\int_\Omega A\cdot Jd\Omega\\ \Gamma_1: A=A_0\end{cases} \tag{7}$$

The magnetic field is discretized into finite space units, by which the nodes are formed. And the solving function *A(x, y, z)* can be expressed by basic function g_i and node function value A_i as follows:

$$\hat{A}=\sum_{i=1}^{N}A_i g_i \tag{8}$$

Where, N is the total number of nodes in the solved region. If the formula (7) is unfolded under rectangular coordinates, the result can be expressed as follows:

$$\begin{aligned}I(A)=&\int_\Omega\frac{1}{2\mu}\left(B_x^2+B_y^2+B_z^2\right)dxdydz\\ &-\int_\Omega\left(A_xJ_x+A_yJ_y+A_zJ_z\right)dxdydz\end{aligned} \tag{9}$$

Where, the discrete forms of B_x 、 B_y and B_z are:

$$\begin{cases}\hat{B}_x=\sum_{i=1}^{n}A_{zi}\dfrac{\partial g_i}{\partial y}-\sum_{i=1}^{n}A_{yi}\dfrac{\partial g_i}{\partial z}\\ \hat{B}_y=\sum_{i=1}^{n}A_{xi}\dfrac{\partial g_i}{\partial z}-\sum_{i=1}^{n}A_{zi}\dfrac{\partial g_i}{\partial x}\\ \hat{B}_z=\sum_{i=1}^{n}A_{yi}\dfrac{\partial g_i}{\partial x}-\sum_{i=1}^{n}A_{xi}\dfrac{\partial g_i}{\partial y}\end{cases} \tag{10}$$

Substituting discrete equations (8) and (10) of $\hat{A}$ and $\hat{B}$ into equation (9), the variational problem of $I\left(A(x,y,z)\right)$ can be transformed into the extremum problem of multivariate function.

$$\frac{\partial I}{\partial A_{wi}}=0 \qquad (w=x,y,z;\ \ i=1,2,\cdots,N) \tag{11}$$

III. Field-Circuit Coupling Model of Saturated Reactor

A. The Field-Circuit Coupling Mathematical Model

Using finite element method and field-circuit coupling method, electromagnetic field of the saturated reactor is analyzed. The excitation in this model is voltage source, and the relation equations of the current in conductor, induced electromotive force and external excitation are established in order to find out the distribution of current and voltage.

The winding circuit equation of the reactor field-circuit coupling model can be described as follows [5]:

$$[U]=[E]-[R][i]-[L]\frac{\partial[i]}{\partial t} \tag{12}$$

Where, $[U]$, $[E]$, $[R]$ and $[L]$ is the node voltage, induced electromotive force, resistance and inductance of the winding correspondingly.

The induced electromotive force of the winding can be expressed like this.

$$\begin{aligned} e&=-\frac{d\psi}{dt}=-\frac{d\left(n\int_S BdS\right)}{dt}\\ &=-\frac{d\left(n\int_\Gamma Adl\right)}{dt}=-n\frac{\partial A}{\partial t}dl \end{aligned} \tag{13}$$

If the length of each turn is l_{turn}, and $N0$ subdivision elements exist in the subdivision region of the winding, the average induction electromotive force of the winding can be expressed as follows:

$$\begin{aligned} E&=-\frac{1}{S}\int_S edS=-\frac{n}{S}\int_S\left(\int_\Gamma\frac{\partial A}{\partial t}dl\right)dS\\ &=-\frac{nl_1}{S}\frac{\partial}{\partial t}\left(\sum_{i=1}^{N_0}A_{\omega i}g_i\right)=[C_e]\frac{\partial[A]}{\partial t} \end{aligned} \tag{14}$$

Where, $[C_e]$ is the coefficients matrix of field-circuit coupling. The circuit equation of the reactor's winding can be described by the following formula:

$$[U]=[C_e]\cdot\frac{\partial[A]}{\partial t}-[R]\cdot[i]-[L]\frac{\partial[i]}{\partial t} \tag{15}$$

Then, the matrix equation of field-circuit coupling can be deduced as follows [6]:

$$\begin{cases} [S][A]+[K][i]=0\\ [C_e]\cdot\dfrac{\partial[A]}{\partial t}-[R]\cdot[i]-[L]\dfrac{\partial[i]}{\partial t}=[U] \end{cases} \tag{16}$$

B. Field-Circuit Coupling Model of The Saturated Reactor in ANSYS

The analysis of the electromagnetic field in ANSYS is based on the basic theory of finite element. The subjects which are to be proposed are divided into finite unites (including a number of nodes), and then magnetic potential and electric potential under certain boundary and initial condition can be solved according to magnetic vector potential and electric scalar potential. Thus the magnetic induction intensity and other related quantities can be derived [7] [8].

The key factors that decide the distribution of the reactor's magnetic field are the turns of *AC* and *DC* windings, the magnitude of current and the size of the iron core.

The clamping parts, fixing parts and other accessories have little effect on the distribution of the reactor magnetic field. Besides, the magnetic leakage in the air should be considered and the air around model is also established. Then finite element mesh for the reactor is conducted.

The 2-D reactor finite element model after meshing is shown in Fig.2 [9].

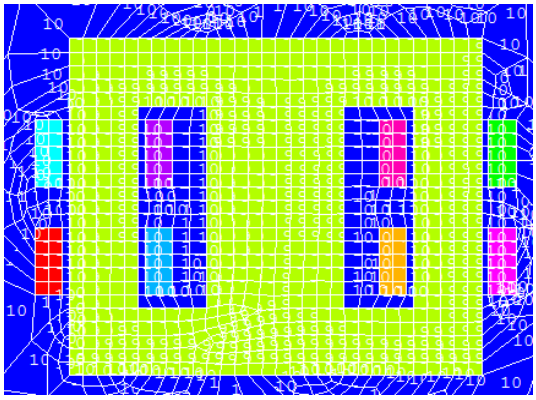

Figure 2. The model of reactor after finite element mesh.

After the real constant is assigned to the winding, and coupling and boundary conditions are added, coupling circuit units established are showed in Fig.3.

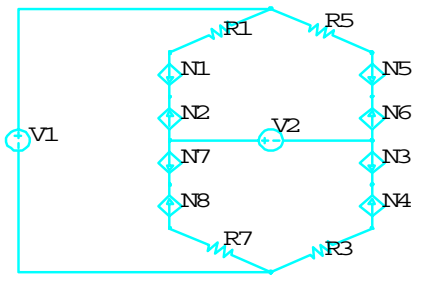

Figure 3. Field-circuit coupling circuit unit.

In Fig.3, *V1* is *AC* voltage source and *V2* is *DC* voltage source. *N1* and *N2* are two sections of the upper left winding. Similarly, *N7* and *N8* 、 *N5* and *N6* 、 *N3* and *N4* are respectively two sections of the other windings. In addition, the two sections of each winding satisfy the condition that current magnitudes are same but directions are opposite. *R1*、*R3*、*R5* and *R7* are the resistances of the four windings correspondingly, and the value is 0.6 ohms. The two branches are connected to the *AC* power source *V1* which are in parallel with each other. At the same time, *DC* control source *V2* is bridge connected to the middle points of the two branches. Therefore, two loops are formed to achieve the controlling effect of DC excitation.

IV. MMATHEMATICAL ANALYSIS AND SIMULATION RESULTS

When the saturated reactor works, the iron core is magnetized by *AC* and *DC* magnetic fields. Furthermore, the most parts of the saturated and unsaturated areas in the basic magnetic curve are covered by the working state of the iron core. In this case, the dynamic hysteresis loop is no longer symmetrical, and the properties of the iron core can't be expressed by the basic magnetizing curve under the condition that *AC* and *DC* excitations co-exist.

In order to facilitate the calculation and analysis, the magnetic properties in this case can be expressed by series of magnetizing curves $B_m = f(H_m, H_y)$. When the fitting of the mathematical model function $H = \phi(B)$ for the *B-H* curve of the *0.35mm* cold-rolled non-oriented silicon steel sheet is conducted, the aim function [10] is shown as follows, in which both the numerator and denominator are polynomial.

$$H = \phi(B) = \frac{\sum_{i=0}^{n} a_i B^i}{B_n + \sum_{j=0}^{n-1} b_j B^j} \tag{17}$$

In order to determine the coefficients a_i and b_i of the aim function, the least square method is adopted. After the fitting of rational fraction, the aim function can be expressed as follows:

$$H = \phi(B) = \frac{a_0 + a_1 B + a_2 B^2 + a_3 B^3}{b_0 + b_1 B + b_2 B^2 + b_3 B^3} \tag{18}$$

Where, $a_0 = 14.14$ ； $a_1 = 147.5$ ； $a_2 = -269.6$ ； $a_2 = 2505.875$ ； $b_0 = 9.709$ ； $b_1 = -7.2$ ； $b_2 = -0.8974$ ； $b_3 = 1.649$

Under the condition *AC* and *DC* excitations co-existing, the total magnetic induction density in the iron core is the sum of *DC* magnetic induction density B_0 and AC magnetic induction density B_1, i.e. $B = B_0 + B_1 = B_0 + B_m \sin \omega t = 1.3 + 0.18 \sin \omega t$ （where, $\omega = 2\pi f$ ， $f = 50Hz$ ）.

The equation for the basic magnetizing curve of the *0.35mm* cold-rolled non-oriented silicon steel sheet can be expressed as follows:

$$H = \phi(B) = \frac{a_0 + a_1 B + a_2 B^2 + a_3 B^3}{b_0 + b_1 B + b_2 B^2 + b_3 B^3} = \frac{14.14 + 147.5B - 269.6B^2 + 2505.875B^3}{9.709 - 7.2B - 0.8974B^2 + 1.649B^3} \tag{19}$$

According to the expression (19), maximum and minimum values of the magnetic field strength are *1398 A/m* and *927 A/m* correspondingly.

Based on the field-circuit coupling model of the saturated reactor, the variations of *B* and *H* in *0.2s-0.3s* are shown in Fig.4 and Fig.5.

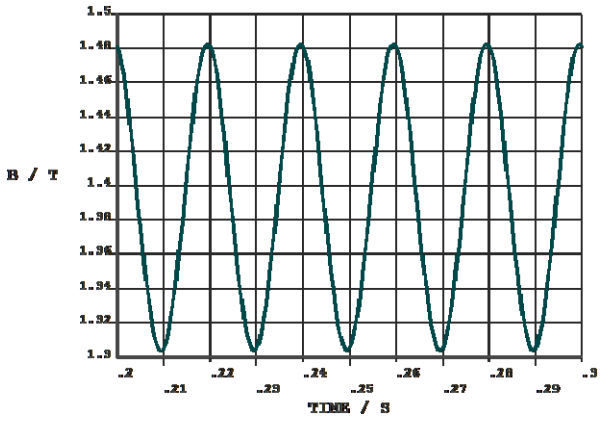

Figure 4. Variation of the magnetic induction density B of the small section.

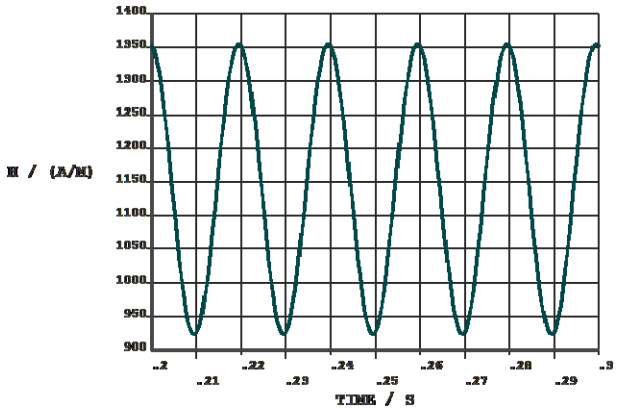

Figure 5. Variation of the magnetic field strength H of the small section.

From the comparison of Fig.3 and Fig.4, the magnetic induction density within the iron core can be expressed as: $B = B_0 + B_1 = B_0 + B_m \sin \omega t = 1.3 + 0.18 \sin \omega t$. The maximum value and minimum value are *1.3T* and 1.48T correspondingly. And for the same reason, the magnetic field strength can be expressed like this: $H = H_0 + H_1 = H_0 + H_m \sin \omega t = 920 + 430 \sin \omega t$. The maximum and minimum values are *920A/m* and *1350A/m* correspondingly.

The comparative analysis on the analytical result and simulation result of the magnetic induction density and magnetic field strength is showed in the following Tab1.

TABLE I. TABLE TYPE STYLES

Physical quantity	Rang	Analytic result	Simulation result	Error
Magnetic induction intensity B(T)	maximum	1.48	1.48	0
	minimum	1.30	1.30	0
Magnetic field strength H(A/m)	maximum	1398	1350	3.56%
	minimum	927	920	0.7%

From Tab.1, errors of the magnetic field strength between the analytic results and the simulation results exist, and the maximum and the minimum are *3.56%* and *0.7%* correspondingly. The reasons are listed as follows [11]:

(1) The analytic expression is derived from the curve fitting for the discrete points on the basic magnetizing curve, therefore, it is reasonable that errors exist between the fitting curve and the practical curve.

(2) In ANSYS simulation, the magnetic induction intensity and magnetic field strength in each unit are different, thus it is inevitable that the magnetic field strength will be different for different units. But both *3.56%* and *0.7%* are within acceptable limits, and can meet the demand of the practical engineering analysis. In conclusion, the analytical expressions have application value.

The working current wave between *0.2-0.3s* are shown as follows:

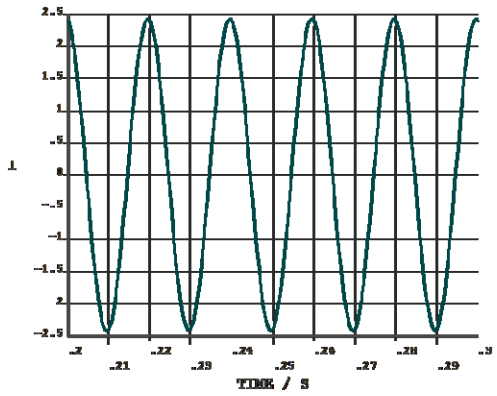

Figure 6. Variation of the working current I.

When the saturated reactor works, DC excitation will inject magnet in one iron core and demagnetize for the other. The DC excitations in the two iron core have the same magnitude and the opposite directions. Because of the nonlinearity of the basic magnetizing curve, distortion of the magnetic field strength will occur in the iron core. But the practical reactor working current is the sum of the currents in the two branches. Its wave is axially symmetric relative to the time axis, and approximately it varies according to the regulation of sin-wave [12]. By adopting the reactor prototype designed for experiment, the harmonic problems brought by the reactor with yoke can be easily solved.

V. CONCLUSION

In this paper, the saturated reactor field-circuit coupling model and the magnetic field are studied. Based on the finite element analysis theory, the accurate *2-D* field-circuit coupling model of the prototype is established in ANSYS. The field-circuit coupling model directly coupled the magnetic field equations and the circuit equations together, and it can reflect the electromagnetic transient process. At the same time, according to the *2-D* field-circuit coupling model, magnetic field and working current in the iron core of the saturated reactor are calculated. The results show that the prototype adopted can efficiently reduce the harmonic injected in the system, by changing the magnetic permeability through superposition of *DC* magnetic field and counteracting the affection produced by nonlinearity though symmetric shunt. The simulation results are corresponded to theoretical analysis on the whole. It can provide foundation for the further study for the saturated reactor other properties.

REFERENCES

[1] Candeo A., Dughiero F., "Numerical FEM models for the planning of magnetic induction hyperthermia treatments with nanoparticles," IEEE Trans. on Magnetics, vol. 45, pp. 1658-1661, March 2009.

[2] Yan Zhaowen, Engineering Electromagnetic Technology and Examples Based on ANSYS 10.0. CA: China Water Conservancy and Hydropower Press, 2006.

[3] Cai Xuansan, Gao Yuenong, Fundamentals and Applications of Controllable Saturated Reactors, Beijing: China Water Conservancy and Hydropower Press, 2008.

[4] Shintaku K., "Magnetic interaction between recording layer and soft underlayer in granular-type perpendicular magnetic recording media with thin intermediate layer," IEEE Trans. on Magnetics, vol. 44, pp. 3503-3506, November 2008.

[5] Yamazaki K., Hyakusoku Y., Muramatsu K., Kitamura H., Fujiwara K., Kobayashi K., "Magnetic disturbance due to the hemispherical hole in the ground for a building at the magnetic test site," IEEE Trans. on Magnetics, vol. 42, pp. 3530-3532, October 2006.

[6] Z.Q. Wang, Z.D. Yin, L.X. Zhou, Z.J. Wang, "Study on controllable reactor magnetic structure and loss based on ANSYS," The 4th IEEE Conference on Industrial Electronics and Applications, Xi'an, 2009, in press.

[7] Zhao Junfeng, Wang Xiulian. "The study of a magnetically controlled saturated reactor core magnetic field in power transformer based on ANSYS," Transactions of Shenyang Ligong University, vol. 26, pp. 58-61, April 2007.

[8] Lu D.W., Wu H.B., Xu X.N., Jin X., "A field distribution of dynamic-link magnetic circuit for room-temperature magnetic refrigeration," IEEE Trans. on Applied Superconductivity, vol. 16, pp. 1554-1557, June 2006.

[9] Xu Yi, Chen Jianye, "Numerical and experimental analysis of magnetically controlled saturated reactor," Converter Technology and Electric Traction, pp. 9-15, March, 2008.

[10] Zhang Liuchen, Xu Song. Application of Finite Element Method in the Electromagnetic Calculation. Beijing: China Railway Press, 1996.

[11] Zhou Lawu, Zhu Yinghao, Zhou Zhiguang, "Regulating range of UHV controlled shunt reactor," Transactions of China Electrotechnical Society, vol. 21, pp. 116-121, December 2006.

[12] Mehasni R, Feliachi M, Latreche M ElH, "Effect of the magnetic dipole interaction on the capture efficiency in open gradient magnetic separation," IEEE Trans. on Magnetics, vol. 43, pp. 3488-3493, August 2007.